

Author's Accepted Manuscript

Lanthanide Luminescence Sensitization via SnO₂
Nanoparticle Host Energy Transfer

Bruno M. Morais Faustino, Peter J.S. Foot, Roman
A. Kresinski



PII: S0022-2313(17)31866-5
DOI: <https://doi.org/10.1016/j.jlumin.2018.10.067>
Reference: LUMIN16015

To appear in: *Journal of Luminescence*

Received date: 4 December 2017
Revised date: 12 October 2018
Accepted date: 12 October 2018

Cite this article as: Bruno M. Morais Faustino, Peter J.S. Foot and Roman A. Kresinski, Lanthanide Luminescence Sensitization via SnO₂ Nanoparticle Host Energy Transfer, *Journal of Luminescence*, <https://doi.org/10.1016/j.jlumin.2018.10.067>

This is a PDF file of an unedited manuscript that has been accepted for publication. As a service to our customers we are providing this early version of the manuscript. The manuscript will undergo copyediting, typesetting, and review of the resulting galley proof before it is published in its final citable form. Please note that during the production process errors may be discovered which could affect the content, and all legal disclaimers that apply to the journal pertain.

Lanthanide Luminescence Sensitization via SnO₂ Nanoparticle Host Energy Transfer

Bruno M. Morais Faustino, Peter J. S. Foot*, Roman A. Kresinski

SEC Faculty, Nanomaterials & Composites Research Group and School of LSPC, Kingston University London, Penrhyn Road, Kingston upon Thames, Surrey KT1 2EE, United Kingdom

*Corresponding author. p.j.foot@kingston.ac.uk

Abstract

Using a sol-gel synthesis method, nanoparticles of SnO₂ doped by a range of lanthanide ions (Ln³⁺) were produced. The UV-visible photoluminescence (PL) emission and excitation spectra were analyzed. Upon excitation of the host oxide at energies above its fundamental bandgap, efficient sensitization of PL emission of all the lanthanide ions was observed. The effects of the Ln³⁺ concentrations and ionic radii on the spectra were discussed and interpreted in terms of likely mechanisms of host-guest energy transfer.

Keywords: tin (IV) oxide nanocrystals; lanthanide; photoluminescence; energy transfer mechanism; ionic radii

1. Introduction

Lanthanides (Ln³⁺) have been exploited for many years as potential luminescent centers. Because their inner-shell 4f orbitals are shielded by filled 5s and 5p valence orbitals, interactions with the surroundings often result in useful luminescent, magnetic and electrical properties with applications in the field of optoelectronic devices such as LED lamps, lasers and optical amplifiers. Despite Ln³⁺ ions being good emissive centers, their 4f and 5d electronic transitions are parity forbidden, so that direct 4f excitation with conventional light sources normally yields only weak luminescence.

However, in Ln-doped wide-band-gap nanosemiconductors (NSCs) such as TiO₂ [1-3], SnO₂ [4-12], ZnO [13-15], etc., lattice defects can give rise to simple configurational mixing caused by the non-centrosymmetric crystal fields, permitting an opposite-parity excited configuration. In addition, because of the larger surface-to-volume ratios in the host NSCs, a range of other physical and chemical properties differ significantly from those in the bulk.

There is considerable interest in the synthesis of Ln-doped wide-band-gap NSC and the optimization of the lanthanides' luminescent properties. Lanthanide host-sensitization studies are numerous, and in many cases, more efficient pathways to Ln excitation are observed, although broad emission lines are often reported, as a result of poor incorporation of Ln³⁺ ions into the NSC crystal lattice. The mechanism of energy transfer (ET) from host to Ln remains a hot topic.

The synthesis and photonic properties of sol-gel derived SnO₂ doped with Ln³⁺ ions were recently reviewed [16]. Amongst this previous work, we have previously reported the observation of intense, well-resolved emission lines from Sm³⁺ by host sensitization in Sm³⁺-doped SnO₂ nanoparticles [4]. A more detailed discussion of the host-sensitization mechanism is presented here for a wider range of lanthanides (Sm³⁺, Eu³⁺, Tb³⁺, Ho³⁺) doped in nanocrystalline SnO₂.

2. Experimental section

The sol-gel synthesis and characterization of the nanoparticulate samples were carried out exactly as previously reported [4] for pure and Sm³⁺-doped SnO₂. Briefly, tin (IV) chloride pentahydrate and 0 to 3 mol % of LnCl₃ (Ln = Sm, Eu, Tb, Ho) were dissolved in methanol and hydrolyzed by aqueous ammonia, forming gels from which Ln-doped SnO₂ nanoparticles were obtained. After washing, drying and annealing at 673 K, the nanocrystallite diameters were determined by powder X-ray diffractometry (XRD) and transmission electron microscopy (TEM) analysis [4] to be in the range 21 - 28 nm.

Photoluminescence studies of thin solid films cast from aqueous suspensions onto quartz slides were carried out at room temperature, using a Varian Cary Eclipse fluorescence spectrophotometer with a 300W Xe lamp excitation source. The spectrometer was calibrated using the fluorescent emission of Rhodamine-B and appropriate correction curves. Measurements were performed with slit settings of 1.5 nm for excitation and emission, at a scan rate of 120 nm min⁻¹.

3. Results and discussion

3.1. SnO_2 Nanocrystals Photoluminescence

Stoichiometric SnO_2 is an insulator, but in its common slightly oxygen-deficient form it behaves as an *n*-type semiconductor with a band gap of 3.6 eV. Point defects in the SnO_2 crystal lattice, either oxygen vacancies or tin interstitials, are responsible for donor states that give rise to several photophysical features [17].

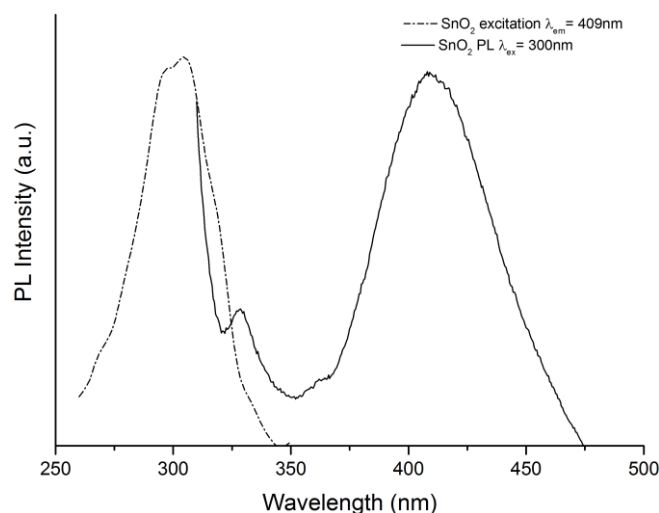


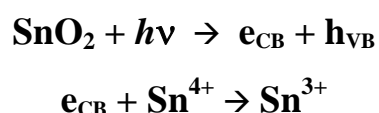
Fig. 1. Normalized solid-state photoluminescent emission and excitation spectra of SnO_2 semiconductor nanocrystals at ambient temperature.

Fig. 1 shows the photoluminescence emission and excitation spectra of SnO_2 nanocrystals, monitoring λ_{em} of 409 nm in the excitation spectrum and λ_{ex} 300 nm in the normalized emission spectrum.

The origin of the visible emission is mainly dependent on the energy band structure of the SnO_2 . Reported calculations show the oxygen *2p* electrons to be tightly bound to the tin *4d* electrons [17,18]. In fact, the valence band (VB) is reported to be mostly made of O *2p* states, with minor contributions from Sn *5s*, *5p*, and a slight contribution from Sn *4d* states due to a small amount of mixing between the Sn *4d* states and O *2p*. The conduction band is mainly of Sn *5s* character with some Sn *5p*, O *2s*, and O *2p* contributions. However, since the energy of the 409 nm emission maximum (3.0 eV) is smaller than the band gap (3.6 eV), emission is unlikely to be the result of direct recombination between a conduction band electron in the Sn *4d* and a hole in the O *2p* valence band. Therefore, as in the cases of common oxide semiconductors such as ZnO [19] and TiO_2 [2, 20-22], emission is a consequence of luminescent centers in the band gap originating from lattice

defects such as oxygen vacancies and Sn interstitials or surface defects such as Sn-Cl or Sn-OH species [23-26].

Intrinsic Sn³⁺ defects may also be generated by reduction of the Sn⁴⁺ ions, and this could occur via a Sn⁴⁺ ion receiving a photoelectron:



Reducing Sn⁴⁺ to the Sn³⁺ state can trap electrons and the corresponding holes may oxidize O²⁻ anions to form O⁻ (trapped hole) or oxygen gas [27].

3.2. Photoluminescence sensitization of Ln³⁺ - doped SnO₂ nanocrystals

In our previous work [4] on sensitization of Sm³⁺ via SnO₂ host energy transfer, evidence of a PL efficiency exceeding that of direct excitation *via* the parity-forbidden *f-f* transitions of Sm³⁺ was reported. The intensity of emission was strongly affected by the excitation wavelength, and the SnO₂ matrix was shown to have an important effect on the energy transfer process. In fact, excitation lines arising from *f-f* transitions were barely detectable, because of the more efficient host-to-dopant pathway of excitation. A maximum efficiency at 1.5 atom % Sm³⁺ (see Fig. 2) was explained on the basis of short-range energy transfer according to Dexter's model [28].

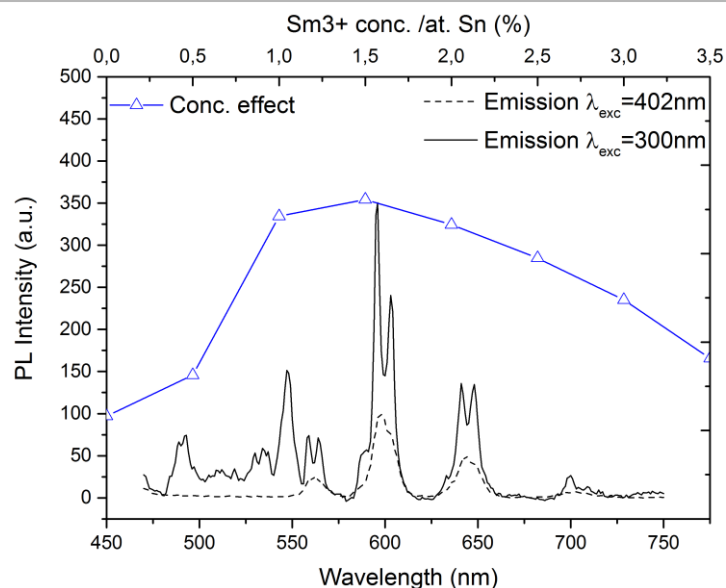


Fig. 2. PL emission spectra of SnO₂:Sm³⁺ via direct excitation at 402 nm and via host-sensitization at 300 nm. The top curve shows the emission of the ⁴G_{5/2}→⁶H_{7/2} transition with varying Sm³⁺ content. Reproduced from Morais Faustino *et al* [4] with permission from Elsevier ©

In an attempt to further verify the nature of energy transfer from the nanoscale semiconductor host to the Ln³⁺, other lanthanides with a range of ionic radii were doped into SnO₂ nanoparticles, and their sensitized emission was studied.

In the case of Eu³⁺, 5 major peaks can be detected in the emission spectra of SnO₂:Eu³⁺ when excited above the SnO₂ band gap: ⁵D₀→⁷F₀ (557 nm), ⁵D₀→⁷F₁ (593 nm), ⁵D₀→⁷F₂ (613 nm), ⁵D₀→⁷F₃ (650 nm), ⁵D₀→⁷F₄ (698 nm). Several other successful photoluminescence sensitization studies on Eu³⁺ have been reported [3, 6, 10, 11, 29-41]. Recent publications on Eu³⁺ sensitization no longer focus on the novelty of emission efficiency but rather on the mechanisms of energy transfer – whether of resonance or non-resonance type [37] – and on the defect states in the nano lattice reportedly contributing to the overall efficiency. The importance of the nano-environment of the lanthanide is further evidenced with europium. For Eu³⁺, the ⁵D₀→⁷F₁ (593 nm) is mostly a magnetic-dipole transition and thus independent of site symmetry, whereas the ⁵D₀→⁷F₂ (613 nm) is an electric-dipole transition and is thus solely allowed at sites of low symmetry with no inversion center [3, 31, 41, 42]. Previous work on Eu³⁺ in rutile-structured SnO₂ by Arai and Adachi [29] has shown strong predominance of the ⁵D₀→⁷F₁ peak, supporting those authors' assertion that the lanthanide ions were in centrosymmetric D_{2h} sites. The observation of five major emission peaks from Eu³⁺ in SnO₂ in the present work is very unusual; the high intensity of the ⁵D₀→⁷F₂ peak indicates that a significant

proportion of the Eu^{3+} is located in non-centrosymmetric (or highly-distorted) sites, but further work will be required to reveal their nature.

Increasing the doping concentration of Eu^{3+} optimizes the emission intensity at 1.5%, beyond which some form of quenching occurs (Fig. 3). In the literature, the optimum amount of Eu^{3+} dopant varies significantly with the type of host material, preparation technique and conditions.

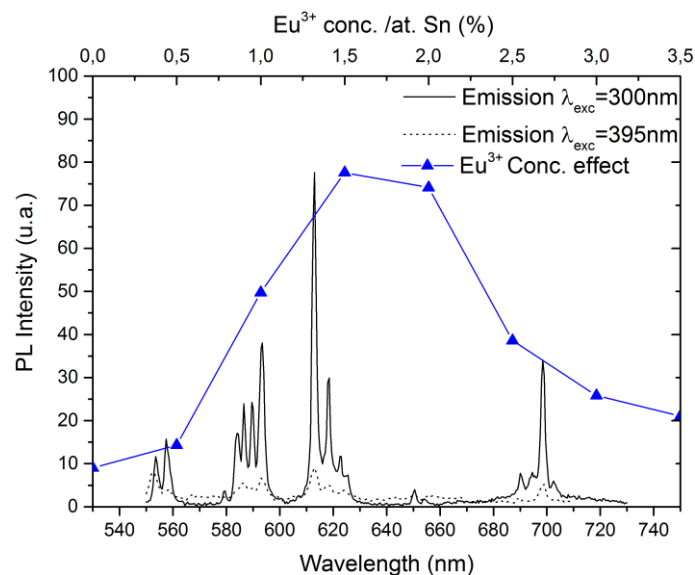


Fig. 3. PL emission spectra of $\text{SnO}_2:\text{Eu}^{3+}$ via direct excitation at 395 nm and via host-sensitization at 300 nm. The top curve shows the emission of the ${}^5\text{D}_0 \rightarrow {}^7\text{F}_2$ transition as a function of Eu^{3+} content.

Likewise, the Tb^{3+} and Ho^{3+} emission is also enhanced upon excitation above the band gap energy of SnO_2 . The resulting emission (490 nm) in Tb^{3+} revealed a maximum intensity at around 2-2.5 atom % Tb^{3+} (Fig. 4 and Fig. 5), and on varying the dopant concentration of Ho^{3+} in $\text{SnO}_2:\text{Ho}^{3+}$ between 0.5-3.5% Ho^{3+} per Sn a maximum efficiency was seen at 2.5% (Fig. 6 and Fig. 7).

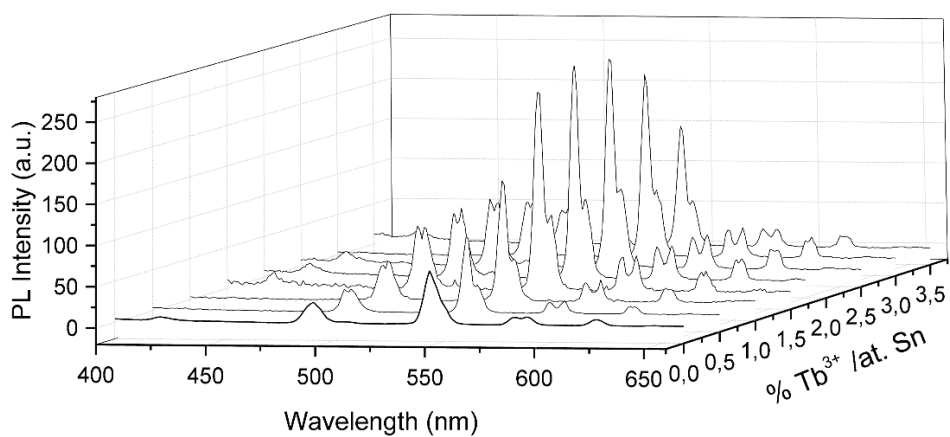


Fig 4. The effect of Tb³⁺ doping concentration on the emission spectra of Tb³⁺ in SnO₂:Tb³⁺ when excited at 300 nm (via host energy transfer). The spectrum at the front is that for direct excitation of the lanthanide ion.

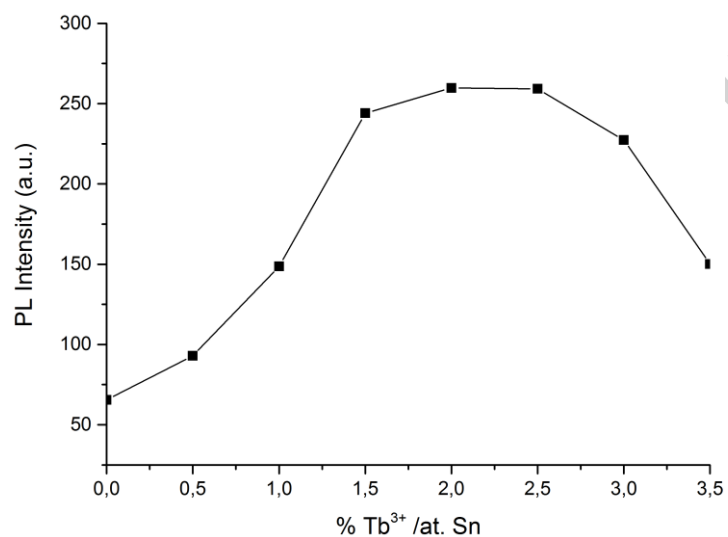


Fig. 5. Intensity of the PL emission from the ⁵D₄ → ⁷F₆ transition in SnO₂:Tb³⁺ as a function of the concentration of Tb³⁺ dopant.

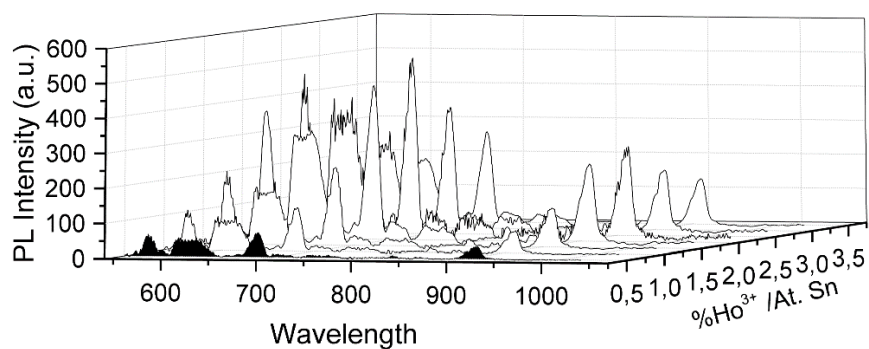


Fig. 6. The effect of Ho^{3+} dopant concentration on the emission spectra of Ho^{3+} in $\text{SnO}_2:\text{Ho}^{3+}$ when excited at 300 nm (via host energy transfer). The spectrum at the front is that for direct excitation of the lanthanide ion.

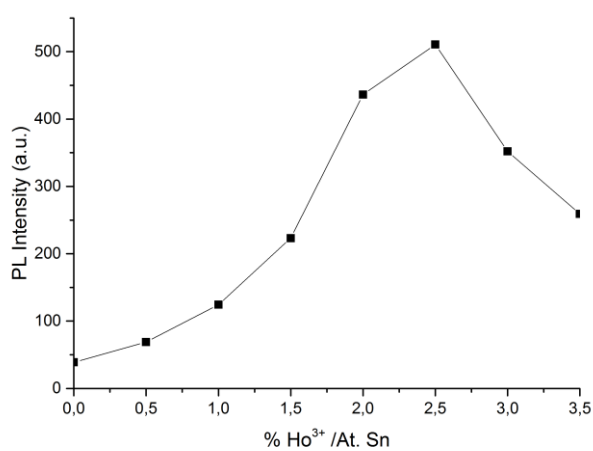


Fig. 7. Intensity of the PL emission from the ${}^5\text{F}_4 \rightarrow {}^5\text{I}_7$ transition in $\text{SnO}_2:\text{Ho}^{3+}$ as a function of concentration of Ho^{3+} dopant.

4. Sensitization energy-transfer mechanism

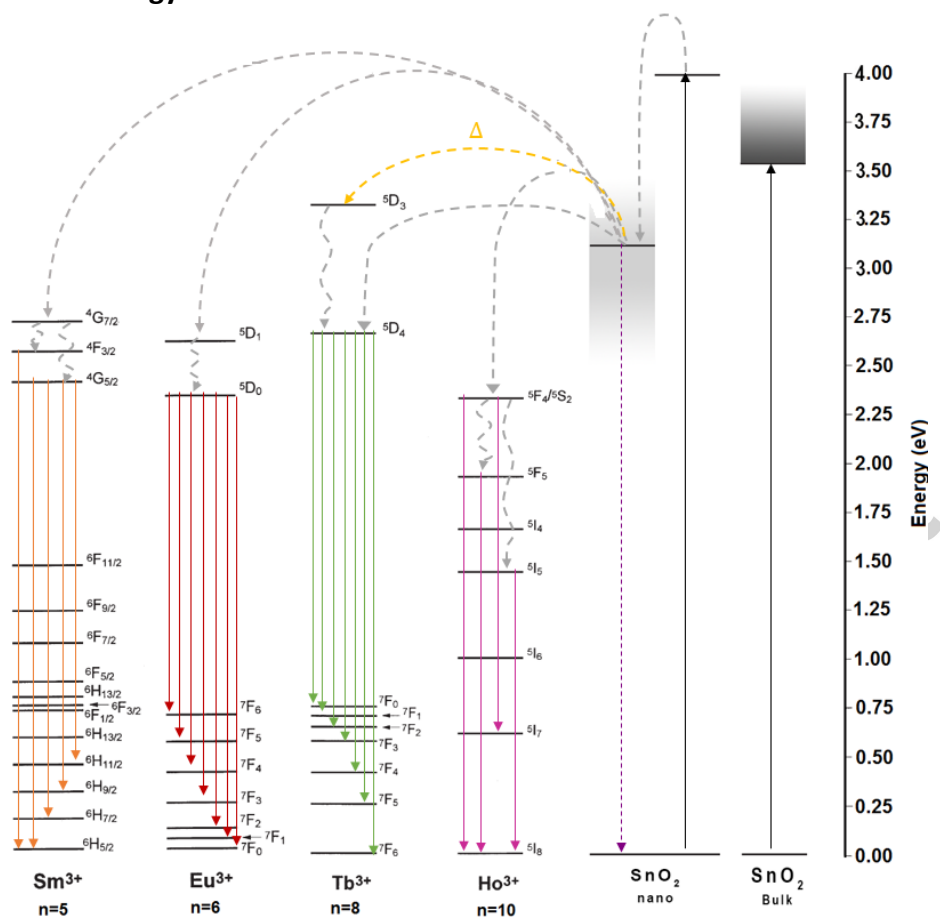


Fig. 8. Suggested mechanism of Ln³⁺ sensitization via host ET mediated by defect states of the SnO₂ nanolattice. (Note: n is the number of valence-shell electrons in each Ln³⁺ ion.)

Fig. 8 illustrates the mechanism of energy transfer from host SnO₂ to Ln³⁺ ions wherein excitation above the band gap of SnO₂ leads to excess electrons in the conduction band, and holes in the valence band. The energy resulting from the recombination of electrons and holes in the host is slightly greater than those of the defect states located high in the band gap [23-26, 28]. The defects are said to be exothermic to the conduction band. The emission spectra of pure SnO₂ nanocrystals show a broad peak centered at 400 nm. The Ln³⁺-doped SnO₂ absorption and excitation spectra feature only the *f-f* lines from Ln³⁺ with no detectable peaks characteristic of SnO₂, indicating a more efficient excitation pathway for Ln³⁺ than direct excitation.

The position of the defect states within the energy gap of the nanosemiconductor is high enough to allow non-radiative energy transfer to an excited state of the neighboring Ln³⁺. Judging by the emission spectra of SnO₂, most of the defect states lie at ca. 3.1eV, although the broadening is most likely due to a collection of states ranging from 2.5 to 3.5 eV. With most defect states lying at around

3.1 eV, they are positioned well above the emissive excited states of all the lanthanides used except Tb^{3+} , for which the $^5\text{D}_3$ emissive state is higher than 3.1 eV, but another emissive state ($^5\text{D}_4$) lies below 3.1 eV. Evidence of this is seen in the expanded spectrum shown in Fig. 9. The 425 nm transition ($^5\text{D}_3 \rightarrow ^7\text{F}_3$) is observed under direct excitation of Tb^{3+} but not in doped samples until about 2% Tb^{3+} . This can be rationalized by considering the importance of the doping effect to the generation of defects due to ionic radii mismatch, thus providing further sensitizing centers at the same level as, or above, $^5\text{D}_3$. The $^5\text{D}_4$ level and its decay to $^7\text{F}_6$, $^7\text{F}_5$, $^7\text{F}_4$ and $^7\text{F}_3$ is also emissive as it lies below the defect state. The above observations support the idea that energy transfer is mediated by oxygen vacancies or other possible defect states in the band gap of SnO_2 . Should the ET process be mainly a result of direct exchange interaction between levels in the conduction band and excited states of Ln^{3+} , the above phenomena would not be seen, and sensitization of the $^5\text{D}_3 \rightarrow ^7\text{F}_3$ transition would occur at Tb^{3+} concentrations as low as 0.5%.

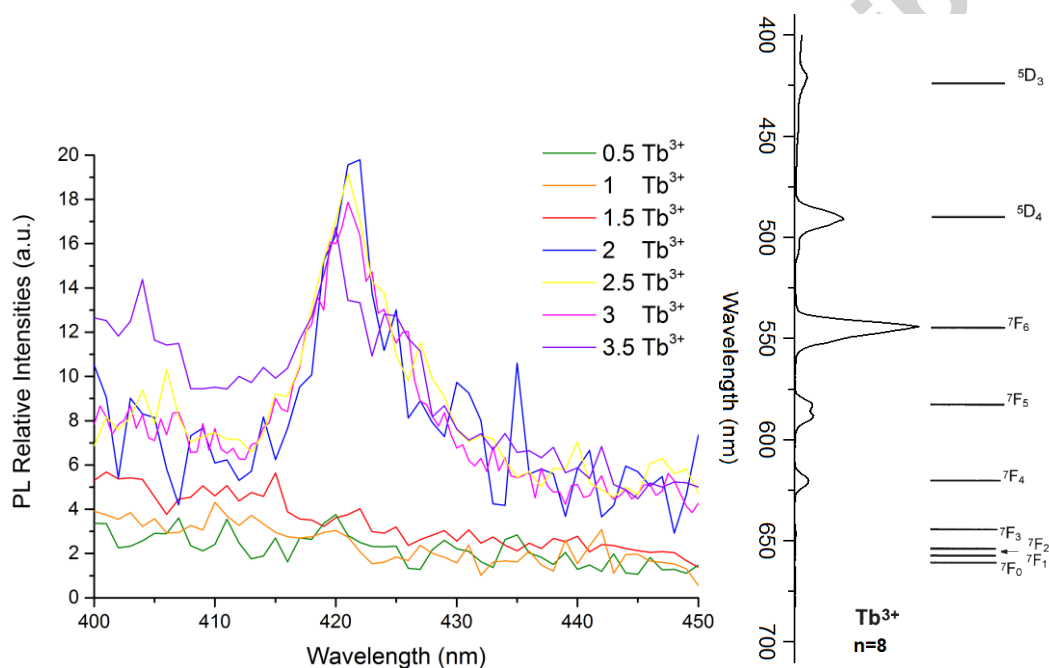


Fig. 9. PL spectra of $\text{SnO}_2:\text{Tb}^{3+}$ for the indicated concentrations of Tb^{3+} (%), expanded in the region of $^5\text{D}_3 \rightarrow ^7\text{F}_3$ Tb emission.

The energy transfer between SnO_2 (conduction band or defects) and Ln^{3+} is thought to be in accordance with Dexter's model [29] for nonradiative ET. This very short-range process ($<10 \text{ \AA}$) requires overlap of wavefunctions between the two species, since the rate of energy transfer by electron exchange is, according to Dexter's model, a function of the separation between the two species. The calculated distances between lanthanides agree with a sensitization process dependent on the ionic radii for every single Ln^{3+} . For example, considering the optimum efficiency at 1.5% in

the case of Sm^{3+} doping, assuming that every fourth atom of Sn^{4+} is substituted by Sm^{3+} in the rutile unit cell, the smallest Sm-Sm distance is 9.2 Å, before quenching predominates and the intensity diminishes. Fig. 10 illustrates the effect of the ionic radii of each Ln^{3+} and the concentrations required to achieve maximum efficiency. A linear trend is consistent with Dexter's model for ET, as the larger the ion the smaller the proportion of Ln^{3+} is necessary to reach the critical distance (in all cases within the <10 Å expected for Dexter-type ET). The emission ratio between the lowest (0.5% Ln^{3+}) and the maximum peak of the most intense transition of each lanthanide demonstrates that smaller ions are more easily sensitized than larger ones (with the exception of a small *inversion*; Eu^{3+} having a smaller ionic radius than Sm^{3+} but being slightly more readily sensitized).

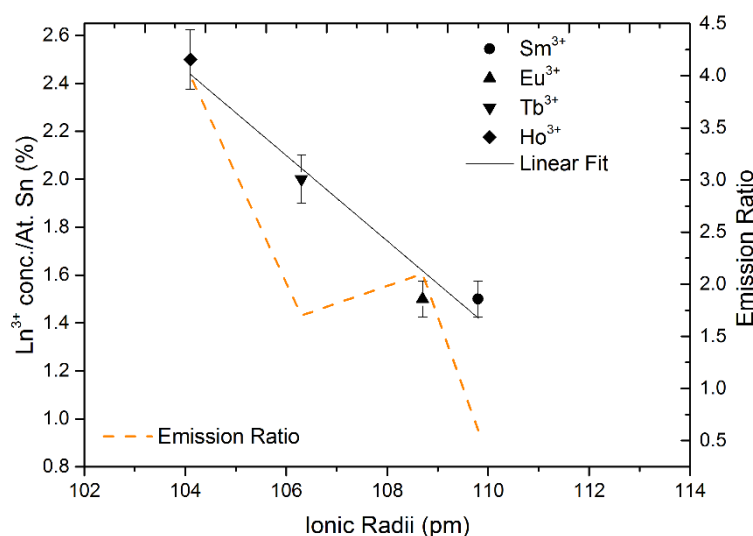


Fig. 10. The concentrations of Ln in doped SnO_2 required to achieve maximum emission from the lanthanide, as a function of the Ln^{3+} ionic radii.

This could be an indication of further modification of the defect state energies, leading to some being below the emissive states due to ionic radii mismatch. However, this remains inconclusive as no obvious alteration of the absorption spectra of SnO_2 is seen with increasing ionic radii of the dopants. No similar studies have been found in the literature with regard to the effect of ionic radii on the emission ratio, although Wang *et al.* [35] found that the introduction of more lanthanide led to greater distortion of the SnO_2 crystal lattice and consequently increased the quenching of the symmetry-allowed transitions. This suggests that larger ionic radii may result in the same effect to some extent. However, in this work the whole range of PL decreased in intensity with larger Ln^{3+} ions, as opposed to the single electric-dipole transitions reported by Wang. Therefore, quenching was most probably a result of Ln^{3+} cross-relaxation; nevertheless, loss of symmetry with increasing dopant concentration may not have been negligible (although seemingly contributing to quenching to an undetectable extent). The quenching results in an equal decrease in emission ratio for all

transitions, whether magnetic or electric-dipole in nature. Equally, improving the crystallinity by increasing the calcination temperature may result in the enhancement of symmetry-allowed transitions [10]. This could ultimately explain Eu^{3+} samples being better sensitized than Tb^{3+} samples, if the emission ratio is not constant for every transition in Eu^{3+} . XRD analysis revealed no significant difference in crystallinity between Tb^{3+} and Eu^{3+} doped nanoparticles.

Indeed, the energy corresponding to the excitation of our nanocrystals at 300 nm (4.1 eV) exceeds the band gap of SnO_2 nanocrystals, which is in turn higher than that of bulk SnO_2 [44]; this is consistent with the notion of the energy being transferred to a higher excited state of the Ln^{3+} ion. Excitation at 300 nm may possibly result in non-radiative transfer to the nearest available excited state of Ln^{3+} . Non-radiative decay of energy from higher to lower excited states generally precedes the visible range emissions from the lowest emissive excited state to the ground state, giving rise to sharp crystal field (CF) emission lines in the PL spectra corresponding to each particular transition. Note that the presence of sharp, well-resolved, CF emission lines is also in agreement with substitutional doping into the SnO_2 lattice, as it reveals the high-level order in the nano-environment at the Ln^{3+} site. Such CF splittings are characteristic of SnO_2 and would vary from nanosemiconductor to nanosemiconductor [3, 6, 11], mostly governed by the unit cell structure of the host.

Despite the significant amount of research on the sensitization of Ln^{3+} ions doped into semiconductor nanocrystals, a comprehensive mechanism for the ET from host to Ln^{3+} is lacking, or at best equivocal in most of the recent literature [2, 6, 19, 21, 35, 45, 46]. There has been repeated mention about the possibility of defect states in the nanosemiconductor playing a crucial role in the ET between host and Ln^{3+} . Indeed, the spectra of nanosemiconductors reveal a broad range of emissive states assigned to defects; however, the understanding of the mechanism of the ET process from the defect energy levels of the host to the dopants has not reached a general consensus yet.

Mukherjee *et al* [47] have summarized the literature on the history of lanthanide sensitization by nanocrystal hosts. Based on supportive evidence from their own experimental data on ZnS Ln^{3+} nanoparticles, the authors agreed with the possibility of Förster (dipole-dipole interaction) and Dexter (exchange interaction) electronic energy transfer mechanisms but also do not discard the likelihood of a third different mechanism dependent on the type of lanthanide. This is consistent with studies by Dorenbos and his co-workers [14, 48-52]. Whether Förster resonance energy transfer (FRET) or exchange interaction dominates, the transfer seems to be extremely dependent on the lanthanide and the host, and hence each system must be considered independently.

Conclusion

Publications on the mechanisms of energy transfer in SnO₂ nanocrystals are relatively scarce. Whilst data herein presented are in good agreement with Dexter-type energy transfer mediated by defects, due to the short inter-dopant distances within the unit cell, a contribution from other processes such as FRET cannot be disregarded, and it may be present to some extent in the case of longer interaction distances between centers several unit cells apart. Therefore, supplementary time-resolved studies on single Ln³⁺-doped SnO₂ nanocrystals will be needed to further investigate the rates of ET in individual systems and to provide greater understanding of the role of defects in the process of Ln³⁺ sensitization.

Acknowledgements

We thank Kingston University London for the provision of a research bursary for BMF. We are also grateful to Prof. D. Phillips (Imperial College London) for helpful comments.

References

- [1] L. Predoana, S. Preda, M. Anastasescu, M. Stoica, M. Voicescu, C. Munteanu, R. Tomescu, D. Cristea, Nanostructured Er³⁺-doped SiO₂-TiO₂ and SiO₂-TiO₂-Al₂O₃ sol-gel thin films for integrated optics, *Opt. Mater.* 46 (2015) 481-490.
- [2] W. Q. Luo, R. F. Li, X. Y. Chen, Host-sensitized luminescence of Nd³⁺ and Sm³⁺ ions incorporated in anatase titania nanocrystals, *J. Phys. Chem.* 113 (2009) 8772-8777.
- [3] W. Luo, R. Li, G. Liu, M. R. Antonio, X. Chen, Evidence of trivalent europium incorporated in anatase TiO₂ nanocrystals with multiple sites, *J. Phys. Chem. C* 112 (2008) 10370-10377.
- [4] B. M. M. Faustino, P. J. S. Foot, R. A. Kresinski, Synthesis and photoluminescent properties of Sm³⁺-doped SnO₂ nanoparticles, *Ceram. Int.* 42 (2016) 18474-18478.
- [5] L. P. Singh, M. N. Luwang, S. K. Srivastava, Luminescence and photocatalytic studies of Sm³⁺ ion doped SnO₂ nanoparticles, *New J. Chem.* 38 (2014) 115-121.
- [6] C. G. Ma, M. G. Brik, V. Kiisk, T. Kangur, I. Sildos, Spectroscopic and crystal-field analysis of energy levels of Eu³⁺ in SnO₂ in comparison with ZrO₂ and TiO₂, *J. Alloy Compd.* 509 (2011) 3441-3451.
- [7] A. C. Yanes, J. Mendez-Ramos, J. del-Castillo, J. J. Velazquez, V. D. Rodriguez, Size-dependent luminescence of Sm³⁺ doped SnO₂ nano-particles dispersed in sol-gel silica glass, *Appl. Phys. B-Lasers and Optics* 101 (2010) 849-854.
- [8] Z. Yuan, D. Li, Z. Liu, X. Li, M. Wang, P. Cheng, P. Chen, D. Yang, Enhanced photoluminescence of Tb³⁺ in SnO₂ film by phosphorus diffusion process, *J. Alloy Compd.* 474 (2009) 246-249.
- [9] D. P. Joseph, P. Renugambal, M. Saravanan, S. P. Raja, C. Venkateswaran, Effect of Li doping on the structural, optical and electrical properties of spray deposited SnO₂ thin films, *Thin Solid Films* 517 (2009) 6129-6136.
- [10] F. Gu, S. F. Wang, M. K. Lü, Y. X. Qi, G. J. Zhou, D. Xu, D. R. Yuan, Luminescent characteristics of Eu³⁺ in SnO₂ nanoparticles, *Opt. Mater.* 25 (2004) 59-64.

- [11] P. S. Chowdhury, S. Saha, A. Patra, Influence of nanoenvironment on luminescence of Eu^{3+} activated SnO_2 nanocrystals, *Solid State Commun.* 131 (2004) 785-788.
- [12] K. Bouras, J. L. Rehspringer, G. Schmerber, H. Rinnert, S. Colis, G. Ferblantier, M. Balestrieri, D. Ihiwakrim, A. Dinia, A. Slaoui, Optical and structural properties of Nd doped SnO_2 powder fabricated by the sol-gel method, *J. Mater. Chem. C* 2 (2014) 8235-8243.
- [13] I. Chauhan, S. Nigam, V. Sudarsan, R. K. Vatsa, Hetero-junction assisted improved luminescence of Eu^{3+} doped ZnO-SnO_2 nanocomposite, *J. Lumin.* 176 (2016) 124-129.
- [14] P. Dorenbos, E. van der Kolk, Lanthanide impurity level location in GaN, AlN and ZnO, *Proc. SPIE* 6473, Gallium Nitride Materials and Devices II, 647313 (February 08, 2007); <https://doi.org/10.1117/12.698977>.
- [15] K. Vanheusden, W. L. Warren, C. H. Seager, D. R. Tallant, J. A. Voigt, B. E. Gnade, Mechanisms behind green photoluminescence in ZnO phosphor powders, *J. Appl. Phys.* 79 (1996) 7983-7990.
- [16] L. Zur, L. T. N. Tran, M. Meneghetti, M. Ferrari, Sol-gel-Derived SnO_2 -based photonic systems, in: L. Klein, M. Aparicio, A. Jitianu (eds.), *Handbook of Sol-Gel Science and Technology*, Springer International Publishing AG, Basel, Switzerland, 2016, pp. 1-19.
- [17] K. G. Godinho, A. Walsh, G. W. Watson, Energetic and electronic structure analysis of intrinsic defects in SnO_2 , *J. Phys. Chem. C* 113 (2009) 439-448.
- [18] T. Yamanaka, J. Mimaki, T. Tsuchiya, The bond character of rutile type SiO_2 , GeO_2 and SnO_2 investigated by molecular orbital calculation, *Zeitschr. Kristall.* 215 (2000) 419-23.
- [19] Y. Du, M. S. Zhang, J. Hong, Y. Shen, Q. Chen, Z. Yin, Structural and optical properties of nanophase zinc oxide, *Appl. Phys. A* 76 (2003) 171-176.
- [20] U. Diebold, The surface science of titanium dioxide, *Surf. Sci. Rep.* 48 (2003) 53-229.
- [21] W. F. Zhang, Z. Yin, M. S. Zhang, Z. L. Du, W. C. Chen, Roles of defects and grain sizes in photoluminescence of nanocrystalline SrTiO_3 , *J. Phys.: Condens. Matter* 11, (1999) 5655-5560.
- [22] W. F. Zhang, M. S. Zhang, Z. Yin, Q. Chen, Photoluminescence in anatase titanium dioxide nanocrystals, *Appl. Phys. B* 70 (2000) 261-265.
- [23] T. W. Kim, D. U. Lee, Y. S. Yoon, Microstructural, electrical, and optical properties of SnO_2 nanocrystalline thin films grown on InP (100) substrates for applications as gas sensor devices, *J. Appl. Phys.* 88 (2000) 3759-3761.
- [24] K. N. Yu, Y. Xiong, Y. Liu, C. Xiong, Microstructural change of nano- SnO_2 grain assemblages with the annealing temperature, *Phys. Rev. B* 55 (1997) 2666-2671.
- [25] A. A. Bolzan, C. Fong, B. J. Kennedy, C. J. Howard, Structural studies of rutile-type metal dioxides, *Acta Cryst. B* 53 (1997) 373-380.
- [26] T. Lin, N. Wang, M. Han, J. Xu, K.-J. Chen, Synthesis, structures and luminescence properties of SnO_2 nanoparticles, *Acta Phys. Sinica* 58 (2009) 5821-5825.
- [27] V. Kumar, O. M. Ntwaeaborwa, J. Holsa, D. E. Motaung, H. C. Swart, The role of oxygen and titanium related defects on the emission of $\text{TiO}_2:\text{Tb}^{3+}$ nano-phosphor for blue lighting applications, *Opt. Mater.* 46 (2015) 510-516.
- [28] D. L. Dexter, A theory of sensitized luminescence in solids, *J. Chem. Phys.* (1953) 21.
- [29] S. J. L. Ribeiro, R. S. Hiratsuka, A. M. G. Massabni, M. R. Davolos, C. V. Santilli, S. H. Pulcinelli, Study of SnO_2 gels by Eu^{3+} fluorescence spectroscopy, *J. Non-Cryst. Solids* 147-148, (1992) 162-166.
- [30] T. Arai, S. Adachi, Difference in photoluminescence properties of $\text{SnO}_2:\text{Eu}^{3+}$ reddish-orange phosphors grown by sol-gel and chemical etching methods, *ECS J. Solid State Sci. Technol.* 3 (2014) R207-R211.
- [31] C. Balasanthiran, B. Zhao, C. Lin, P. S. May, M. T. Berry, J. D. Hoefelmeyer, Self-limiting adsorption of Eu^{3+} on the surface of rod-shape anatase TiO_2 nanocrystals and post-synthetic sensitization of the europium-based emission, *J. Colloid Interfac. Sci.* 459 (2015) 63-69.

- [32] T. Arai, S. Adachi, Simple wet chemical synthesis and photoluminescence characterization of $\text{SnO}_2:\text{Eu}^{3+}$ reddish-orange phosphor, *J. Lumin.* 153 (2014) 46-53.
- [33] N. Bajpai, S. A. Khan, R. S. Kher, N. Bramhe, S. J. Dhoble, A. Tiwari, Thermoluminescence investigation of sol-gel derived and γ -irradiated $\text{SnO}_2:\text{Eu}^{3+}$ nanoparticles, *J. Lumin.* 145 (2014) 940-943.
- [34] M. Nogami, T. Enomoto, T. Hayakawa, Enhanced fluorescence of Eu^{3+} induced by energy transfer from nanosized SnO_2 crystals in glass, *J. Lumin.* 97 (2002) 147-152.
- [35] G. Wang, Y. Yang, Q. Mu, Y. Wang, Preparation and optical properties of Eu^{3+} -doped tin oxide nanoparticles, *J. Alloy Compd.* 498 (2010) 81-87.
- [36] A. Gupta, N. Brahme, D. Prasad Bisen, Electroluminescence and photoluminescence of rare earth (Eu, Tb) doped Y_2O_3 nanophosphor, *J. Lumin.* 155 (2014) 112-118.
- [37] S. Dabboussi, H. Elhouichet, H. Ajlani, A. Moadhen, M. Oueslati, J. A. Roger, Excitation process and photoluminescence properties of Tb^{3+} and Eu^{3+} ions in SnO_2 and in SnO_2 : porous silicon hosts, *J. Lumin.* 121 (2006) 507-516.
- [38] H. Elhouichet, L. Othman, A. Moadhen, M. Oueslati, J. A. Roger, Enhanced photoluminescence of Tb^{3+} and Eu^{3+} induced by energy transfer from SnO_2 and Si nanocrystallites, *Mater. Sci. Eng.: B* 105 (2003) 8-11.
- [39] J. del-Castillo, A. C. Yanes, J. J. Velázquez, J. Méndez-Ramos, V. D. Rodríguez, Luminescent properties of $\text{Eu}^{3+}-\text{Tb}^{3+}$ -doped $\text{SiO}_2-\text{SnO}_2$ -based nano-glass-ceramics prepared by sol-gel method, *J. Alloy Compd.* 473 (2009) 571-575.
- [40] P. Y. Poma, K. U. Kumar, M. V. D. Vermelho, K. Serivalsatit, S. A. Roberts, C. J. Kucera, J. Ballato, L. G. Jacobsohn, C. Jacinto, Luminescence and thermal lensing characterization of singly Eu^{3+} and Tm^{3+} doped Y_2O_3 transparent ceramics, *J. Lumin.* 161 (2015) 306-312.
- [41] J. del-Castillo, A. C. Yanes, S. Abé, P. F. Smet, Site selective spectroscopy in $\text{BaYF}_5:\text{RE}^{3+}$ (RE= Eu, Sm) nano glass-ceramics, *J. Alloy Compd.* 635 (2015) 136-141.
- [42] K. Binnemans, *Coord. Chem. Rev.* 295 (2015) 1-45.
- [43] X. Y. Chen, G. K. Liu, The standard and anomalous crystal-field spectra of Eu^{3+} , *J. Sol. State Chem.* 178 (2005) 419-428.
- [44] Y. Zhang, B. Fluegel, M. C. Hanna, A. Mascarenhas, L.-W. Wang, Y. J. Wang, X. Wei, Impurity perturbation to the host band structure and recoil of the impurity state, *Phys. Rev. B* 68 (2003) 075210.
- [45] S. Das, V. Jayaraman, SnO_2 : a comprehensive review on structures and gas sensors, *Prog. Mater. Sci.* 66 (2014) 112-255.
- [46] Y. Liu, W. Luo, H. Zhu, X. Chen, Optical spectroscopy of lanthanides doped in wide band-gap semiconductor nanocrystals, *J. Lumin.* 131 (2011) 415-422.
- [47] P. Mukherjee, C. M. Shade, A. M. Yingling, D. N. Lamont, D. H. Waldeck, S. Petoud, Lanthanide sensitization in II-VI semiconductor materials: A case study with terbium (III) and europium (III) in zinc sulfide nanoparticles, *J. Phys. Chem. A* 115 (2011) 4031-4041.
- [48] P. Dorenbos, Systematic behaviour in trivalent lanthanide charge transfer energies, *J. Phys.: Condens. Matter* 15 (2003) 8417.
- [49] P. Dorenbos, $f \rightarrow d$ transition energies of divalent lanthanides in inorganic compounds, *J. Phys.: Condens. Matter* 15 (2003) 575-594.
- [50] P. Dorenbos, Lanthanide charge transfer energies and related luminescence, charge carrier trapping, and redox phenomena, *J. Alloy. Compd.* 488 (2009) 568-573.
- [51] P. Dorenbos, E. van der Kolk, Location of lanthanide impurity energy levels in the III-V semiconductor $\text{Al}_x\text{Ga}_{1-x}\text{N}$ ($0 \leq x \leq 1$), *Opt. Mater.* 30 (2008) 1052-1057.
- [52] P. Dorenbos, E. van der Kolk, Location of lanthanide impurity levels in the III-V semiconductor GaN, *Appl. Phys. Lett.* 89 (2006) 061122.

HIGHLIGHTS:

- SnO_2 nanocrystals are doped with a range of lanthanide ions (Ln = Sm, Eu, Tb, Ho)
- Photoluminescent properties show efficient host-guest sensitization
- Concentration dependence suggests Dexter energy transfer from O vacancies to dopant
- Largest Ln ions need lower concentrations to reach maximum luminescence

Accepted manuscript